*International Journal of Minerals, Metallurgy and Materials*
*Volume 23, Number 6, June 2016, Page 723*
**DOI: 10.1007/s12613-016-1286-0**

# Graphene-reinforced aluminum matrix composites prepared by spark plasma sintering

*Wen-ming Tian, Song-mei Li, Bo Wang, Xin Chen, Jian-hua Liu, and Mei Yu*

School of Materials Science and Engineering, Beihang University, Beijing 100191, China
(Received: 3 September 2015; revised: 28 November 2015; accepted: 6 January 2016)

**Abstract:** Graphene-reinforced 7055 aluminum alloy composites with different contents of graphene were prepared by spark plasma sintering (SPS). The structure and mechanical properties of the composites were investigated. Testing results show that the hardness, compressive strength, and yield strength of the composites are improved with the addition of 1wt% graphene. A clean, strong interface is formed between the metal matrix and graphene via metallurgical bonding on atomic scale. Harmful aluminum carbide ($Al_4C_3$) is not formed during SPS processing. Further addition of graphene (above 1wt%) results in the deterioration in mechanical properties of the composites. The agglomeration of graphene plates is exacerbated with increasing graphene content, which is the main reason for this deterioration.

**Keywords:** metal matrix; composites; spark plasma sintering; aluminum; graphene; mechanical properties

## 1. Introduction

Graphene is a single layer of a two-dimensional lattice assembled from $sp^2$-hybridized carbon atoms, and has attracted considerable attention in recent years because of its excellent thermal, electrical, and mechanical properties [1–2]. Single layer graphene has a fracture strength of 130 GPa, a Young's modulus of 1 TPa, a low density of 1.06 g/cm$^3$, and a larger specific surface area [3], making it an excellent reinforcement for metal matrix composites [4]. To date, a number of studies have reported the successful fabrication of graphene-reinforced metal matrix composites; this modification was demonstrated to have a positive effect on the mechanical properties of the final products [4–7]. Jeon *et al.* [8] also reported the enhanced thermal conductivity of an aluminum matrix due to the addition of graphene.

The poor wettability of the graphene/metal interface usually results in the weak interface adhesion and reduces the mechanical performance of the metal matrix due to the tremendous differences in physical and chemical properties of metal and graphene [4–6,8]. In addition, graphene is more difficult to disperse than other reinforcements, owing to its greater interfacial contact area [4]. The homogeneous dispersion of graphene throughout the metal matrix is a key issue during the preparation of composites. Traditional fabrication methods, such as stir casting, cannot overcome this problem. To achieve the homogeneous dispersion of graphene in metal matrices, dispersion methods based on mechanical milling (e.g., ball milling) have been developed [4–7]. Some liquid dispersion techniques (e.g., pre-stir powders in liquid) were also adopted in some studies [9].

The techniques to fabricate graphene-metal matrix composites are generally based on powder metallurgy. The usual processing routes of graphene-metal matrix composites include compacting and sintering mixed powders, or the bulk composites are sintered by hot isostatic pressure in one step [4–6,9–10]. Meanwhile, a subsequent hot extrusion is usually needed to improve the densification of the composites, because it is difficult to prevent the formation of micro-holes in composites after sintering [6,9]. Bartolucci *et al.* [4] fabricated a 0.1wt% aluminum–graphene composite using ball milling, hot isostatic pressing, and extrusion. Although the aluminum-graphene composite in their study

Corresponding author: Song-mei Li E-mail: songmei_li@buaa.edu.cn

showed the increased hardness, its strength and ductility decreased significantly due to the formation of $Al_4C_3$ caused by the long period of ball milling and high temperature (550°C) sintering. Li *et al.* [6] adopted an improved fabrication technique, i.e., cryomilling (at −181°C), followed by hot isostatic sintering and extrusion at a relatively lower temperature (300°C). This technique effectively prevented the formation of $Al_4C_3$ at the graphene/aluminum interface, and resulted in a significant increase in tensile strength without loss of ductility when the addition of graphene was 0.5wt%. However, this method was time-consuming (total time is over 26 h). Pérez–Bustamante *et al.* [5] studied the effects of milling time and hot isostatic sintering time on the mechanical properties of aluminum-graphene composites. The hardness of the composites increased with increasing graphene content and obtained a maximum at 1wt% graphene content. The hardness also increased with increasing ball milling time, due to the fact that prolonging the milling time could increase the amorphous fraction of graphene and improve the interface adhesion between graphene and metal. The authors concluded that the best processing parameters were 5 h milling and 2 h sintering. Dutkiewicz *et al.* [10] prepared the graphene-reinforced copper matrix composites using vacuum uniaxial hot pressing ball milled mixtures and studied the effects of graphene size on the mechanical properties of the composites. Smaller graphene plates had a better reinforcement effect because the larger plates agglomerated more easily.

Meanwhile, the fabrication techniques mentioned above are generally quite time-consuming and not cost effective to prepare bulk composites, due to their long periods of milling and sintering as well as their complicated processing routes. In addition, mechanical milling will increase the density of defects (such as prism planes) on graphene plates. The long period (dozens of hours), high pressure (hundreds of MPa), and high temperature during compaction and sintering of the powders will increase the formation of detrimental metallic carbides and deteriorate the mechanical properties of the composites [4–6,8,10]. Additionally, some kinds of dispersants such as stearic acid are always added during ball milling; these are difficult to remove thoroughly from the mixtures during hot isostatic pressing, and thus result in the formation of $Al_4C_3$ and micro-holes. These defects are harmful to the mechanical properties of the composites [4–6]. To address these problems, Jeon [8] *et al.* developed a friction stir processing method to fabricate metal-graphene composites and achieved the improved thermal conductivity and better tensile strength. However, this method is not suitable to prepare bulk metal-graphene composites, due to its mechanism limitations.

Spark plasma sintering (SPS) can provide a time-saving, low-temperature, low-pressure and high-quality method for the fabrication of composites [11–12]. However, to date, few studies have used SPS to prepare graphene-reinforced metal matrix composites. In the present work, graphene-reinforced 7055 aluminum matrix composites were prepared by SPS. The metal powders and graphene plates were pre-dispersed in an ultrasonic acetone bath. The effects of graphene content on the mechanical properties of the composites were also investigated.

## 2. Experimental

### 2.1. Materials and processing

7055 aluminum alloy powder with a diameter of 50 μm was used as the metal matrix material. The graphene plates were chemically reduced from graphene oxide (GO) suspension by hydrazine, and the GO was prepared via the Hummer's method. The whole reduction process took place in an ultrasonic bath. The 0, 1wt%, 3wt%, and 5wt% graphene plates were wet-blended with 7055 aluminum powders in an acetone solution in an ultrasonic bath for 4 h. The mixed powders were vacuum dried at 50°C for 24 h. Then the dried mixed powders were loaded in a cylindrical graphite die with an inner diameter of 15 mm for SPS processing. The SPS experiments were carried out at 400°C in vacuum with a 1 min dwell time and a heating rate of 50°C/min. A uniaxial pressure of 50 MPa was applied during the whole SPS process. The samples were cooled naturally after the sintering period.

### 2.2. Characterization

Vickers hardness tests were performed by a 300 g weight in a 10 s load dwell time. The materials were machined into cylinders (ϕ4 mm × 10 mm) to test the compressive properties. The compressive tests were performed at a 0.3 mm/min constant compression rate. X-ray diffraction (XRD) analysis was used to study the phase compositions of the sintered samples in a $2\theta$ range of 20° to 90° at a step size of 0.02° using Cu $K_\alpha$ radiation. The Raman spectra of the composites and pure graphene were measured in an incident laser light at 633 nm wavelength and 4 × 4 $\mu m^2$ spot size. The back scattered electron images (BEI) of sintered composites were observed by scanning electron microscope (SEM) with an accelerating voltage of 25 kV. The interfaces between aluminum and graphene were investigated by transmission electron microscopy (TEM) with an accelerating voltage of 200 kV.

## 3. Results and discussion

### 3.1. Raman spectra analysis

Fig. 1 shows the Raman spectra of the chemically reduced graphene plates and sintered composites. The Raman spectra present the characteristic signals of multilayer graphene with peaks of D, G, and 2D bands [5]. The intensity of peaks increases significantly with graphene content, and reaches the highest value for pure graphene. Fig. 1 also shows that the G band of the composites exhibits a red shift relative to that of pure graphene (1573 $cm^{-1}$). Also, the red shift of G band becomes more severe with increasing graphene content (1wt% at 1586 $cm^{-1}$, 3wt% at 1598 $cm^{-1}$, and 5wt% at 1610 $cm^{-1}$). This indicates a relatively poor electronic interaction between graphene and the metal matrix, i.e., more severe agglomeration and coalescence for graphene plates in the composites with higher graphene contents [2,13–14]. The severe agglomeration of plates will deteriorate the physical properties of graphene in composites, due to the weak interfaces between the reinforcements. The intensity ratio of D band and G band ($I_D/I_G$) indicates the disordered structure and defect density of carbon [9–10]. The values of $I_D/I_G$ for the 1wt%, 3wt%, and 5wt% graphene composites are 1.387, 1.457, and 1.599, respectively. The increased $I_D/I_G$ value can be ascribed to the increased defects, the disordered structure on graphene plates, and the restoration of numerous graphic domains [2,5,8]. The intensity ratio of 2D band and G band ($I_{2D}/I_G$) also can be used to estimate the defect density on graphene plates [14–15]. Also, the decreased value of $I_{2D}/I_G$ (0.164 for 1wt%, 0.150 for 3wt%, and 0.147 for 5wt%) demonstrates the increased defect density within the graphene plates at higher contents.

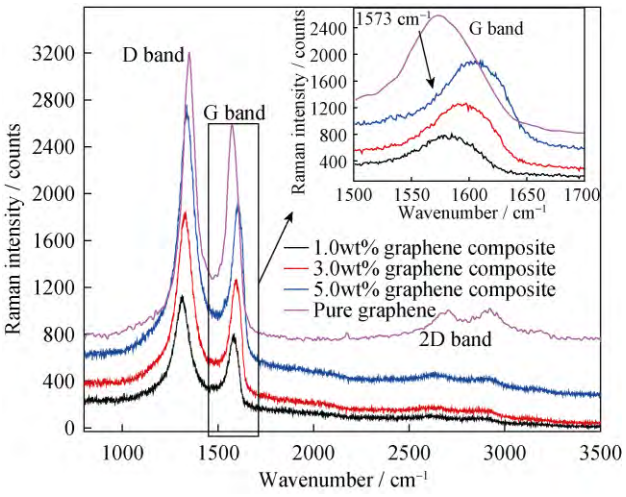


**Fig. 1. Raman spectra of the sintered composites and pure graphene.**

The Raman spectra analysis showed that the agglomeration and coalescence of graphene plates in the composites became more severe with a higher graphene content; more defects and disordered structures were also generated within the plates. This promoted the formation of detrimental metallic carbides and was harmful to the mechanical properties of the composites.

### 3.2. Mechanical properties

Fig. 2 shows that the Vickers hardness increases from Hv 131.5 (7055 aluminum alloy) to Hv 151.2 after the addition of 1wt% graphene plates. However, further addition of graphene is detrimental to the Vickers hardness. Obviously, the hardness of composite with 3wt% graphene (Hv 128.3) is lower than that of the pure alloy and reaches the lowest value at 5wt% graphene (Hv 98.6). Typical compressive strength curves and the correlative results of the sintered composites are shown in Fig. 3. The composite with an addition of 1wt% graphene significantly improves the mechanical properties. The yield strength and compressive strength increase by 34.9% and 22.1%, respectively, compared to pure 7055 aluminum alloy. Firstly, the strengthening effect can be attributed to the super-high strength of graphene and the homogeneous dispersion of reinforcements in the alloy matrix. Secondly, as other dispersoids, such as AlN, $B_4C$, SiC, and carbon nanotubes, graphene plates can also inhibit grain growth by grain boundary pinning [16–23]. A clean and strong interface between the metal matrix and reinforcement is also necessary. Meanwhile, the graphene plates in the metal matrix can obstruct the migration of dislocations and vacancies [6,24]. Therefore, the decreased compressive strain of the 1wt% graphene composite can be attributed to the obstruction of dislocations and vacancies. Both the compressive strength and strain decrease significantly when the graphene content

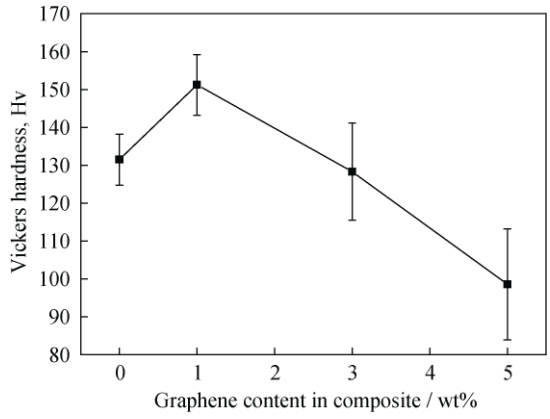


**Fig. 2. Vickers hardness of the sintered composites with different graphene contents.**

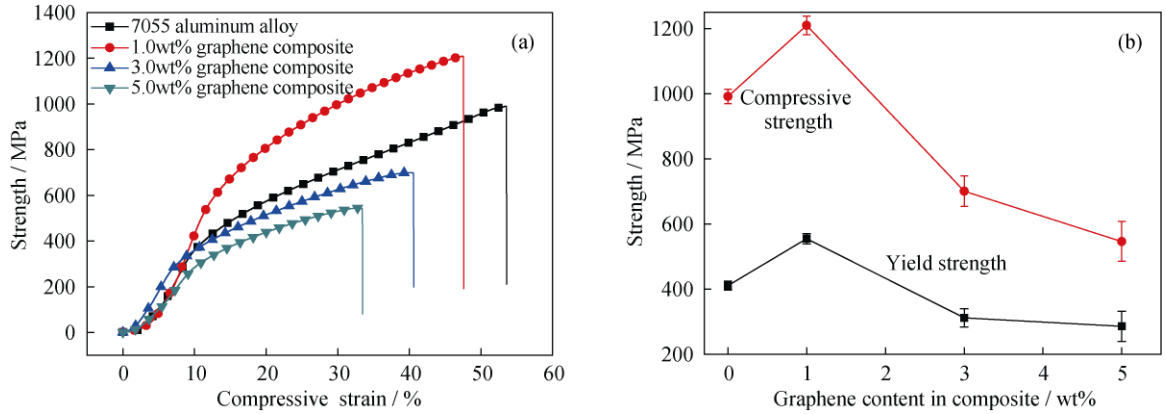


**Fig. 3. Typical compressive strength curves (a) and correlative compressive test results (b) of the sintered composites with different graphene contents.**

reaches 3wt% and 5wt%, because the agglomeration and coalescence of the graphene plates become more severe at higher contents, as illustrated by Raman spectral analysis. Even a low mass fraction may result in a high volume fraction, due to the low density of graphene; with the addition of relatively large metal powders (50 μm), the severe agglomeration becomes inevitable at higher graphene contents. The agglomerated graphene plates may transform into graphite and lose their super-high strength after SPS sintering, and the weak interfaces between the agglomerated plates can be broken easily under the compressive load. Therefore, both the compressive strength and strain decrease significantly when the graphene content reaches 3wt% and 5wt%.

The agglomeration of graphene plates and the deteriorated mechanical properties of the composites caused by the excessive addition of graphene to the metal matrix have been reported in many studies by Raman test [5,8,10,12]. The interfaces between the agglomerated graphene plates are usually weak because of the plicated nature of graphene. Cracks and gaps usually exist between the agglomerated plates and thus reduce the bounding energy at interface, which deteriorate the mechanical properties of the composites [5–8]. In addition, some agglomerated graphene plates can turn into graphite and lose their excellent mechanical properties. Different researchers give the different optimal addition contents. Li *et al.* [6] reported that the best content of graphene in aluminum composites was 0.5wt%, and the tensile strength would decrease significantly above this content due to the gaps and voids between the agglomerated plates. Pérez–Bustamante *et al.* [5] found that the hardness of aluminum matrix composites increased with increasing graphene content; the highest hardness was obtained at 1wt% content. Dutkiewicz *et al.* [10] claimed that the hardness of the composites increased by 50% and the electrical resistivity decreased by 30% with the addition of 1wt% graphene nano-plates to a copper matrix. The further addition of graphene (over 2wt%) resulted in the thickening of some plates to dozens or hundreds of nanometers, which indicated a severe agglomeration of graphene. Graphene plates with such thicknesses would turn into graphite and lose their excellent mechanical properties, reducing the hardness of the composites significantly. The optimal addition amount of graphene depended on the processing technique, powder size, and metal type. Tang *et al.* [2] fabricated a 0.94wt% graphene-reinforced copper-nickel composite, the tensile strength of composites increased significantly and the ductility decreased compared to pure copper. Again, the further addition of graphene resulted in gaps between plates and reduced both of the strength and ductility. Li *et al.* [6] calculated that the theoretical optimal addition content of graphene to aluminum was 4wt%; however, it is difficult to add more than 1wt%. This discrepancy can be explained by the fact that their calculation fails to take some certain factors into consideration, such as the fact that graphene plates are never uniformly dispersed along the grain (powder) boundaries without any agglomeration in the aluminum matrix. Additionally, the aluminum grains are never homogeneous in size, nor regular in morphology [6].

### 3.3. Microstructure and XRD characterization

BEI images and bright field TEM images of the sintered composites are shown in Fig. 4. The graphene plates are well distributed in the metal matrix, indicating good dispersion of the reinforcements, which is beneficial to the mechanical strength of the composites. TEM images in Figs. 4(b)-(d) show that no crevices or abrupt boundaries are formed between the graphene plates and the metal matrix; a clear and clean transition region is also observed at the interface zone. This demonstrates that the graphene and metal matrix have clean and strong interfaces that undergo

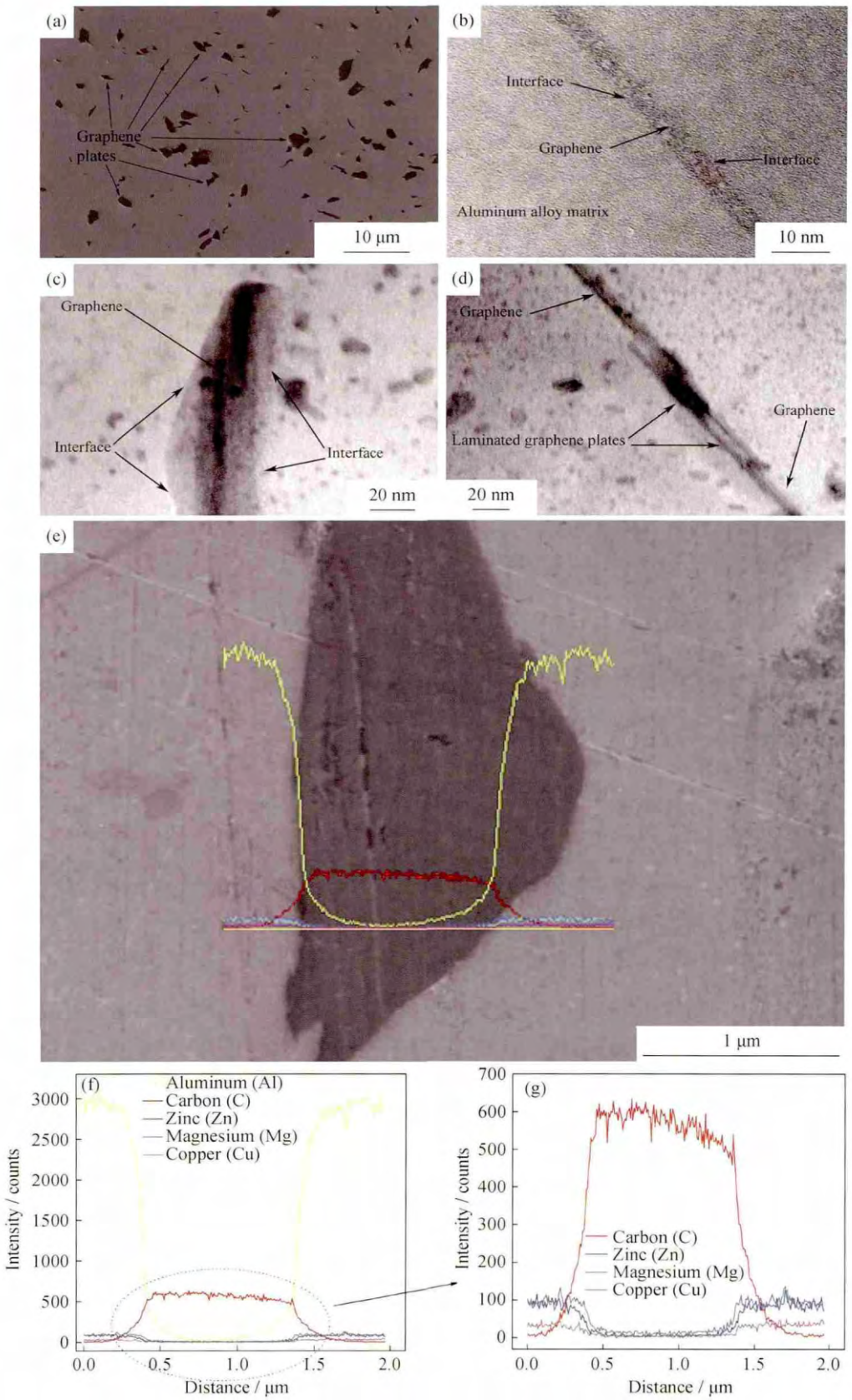


**Fig. 4. BEI image of the 1wt% graphene composite (a), bright field TEM images of graphene plates in the 1wt% graphene composite ((b) and (c)), bright field TEM image of laminated graphene plates in the 3wt% graphene composite (d), and EDS line scan results of graphene plates in the composites ((e), (f), and (g)).**

metallurgical bonding at atom scale, indicating the intercalation between carbon atoms and aluminum atoms. The same kind of high quality interface between the graphene plates and metal matrix was also observed in Refs. [2,4–6,9] by TEM. In addition, the thickness of a single graphene plate (Fig. 4(b)) in the 1wt% composite is smaller than that of the laminated plate (Fig. 4(d)) in the 3wt% composite; this indicates that more severe agglomeration occurs at higher graphene contents. The result of EDS line scan test, presented in Figs. 4(e)-(g), proves that darker phases in Fig. 4(a) are graphene. The smooth element distribution lines of carbon and aluminum also indicate good adhesion between the metal and graphene, and thus a high quality interface. This clean, strong interface is an effective transition layer to transfer load from the metal matrix to the graphene plates.

For the composites reinforced by carbon nanotubes and graphene, the formation of aluminum carbide ($Al_4C_3$) is difficult to prevent during preparation. $Al_4C_3$ is the most energetically favorable stoichiometry of aluminum carbides, and it is harmful to the mechanical properties of composites; its formation shows a strong dependence on the processing temperature, and becomes inevitable when the fabrication temperature is above 500°C [4–6,9]. It preferentially grows on the high surface free energy prismatic planes of carbon. This has been seen in the conventional sized carbon fibers and is deleterious to the strength of composites [4]. The highly stable defect-free graphitic planes on carbon nanotubes or graphene do not react with aluminum to form aluminum carbide even at very high temperatures in molten aluminum. Carbide formation will be promoted at defects in the graphitic planes (which exposes the prism planes) at the tube ends and on the amorphous carbon coating at temperatures below the melting point of aluminum [4–6]. A higher temperature and higher density of defects on the graphene surface will promote the formation of $Al_4C_3$. XRD analysis results for pure 7055 aluminum alloy and composites are shown in Fig. 5. The characteristic peaks of $Al_4C_3$ are not detected; other kinds of metallic carbides are also absent. Even though the graphene content increases to 3wt% and 5wt%, and the graphite is detected, $Al_4C_3$ is still absent. This can be attributed to the low sintering temperature (400°C) and non-milling blending process. The XRD test also proves the severe agglomeration and formation of graphite in the 3wt% and 5wt% composites, because the characteristic peak of graphite is detected in both these composites. SPS processing also has a specific surface cleaning effect [11–12,24–25]; it not only removes the residual oxygen-containing functional groups and defects remained on the graphene plates, but also effectively eliminates the oxide films and adsorbed contaminants on the metal powders. With the addition of the electrical activation effects of SPS during sintering, a strong, clean, atomic intercalated and $Al_4C_3$-free interface is formed between the graphene and the metal matrix. This is desirable for a high-performance aluminum-graphene composite.

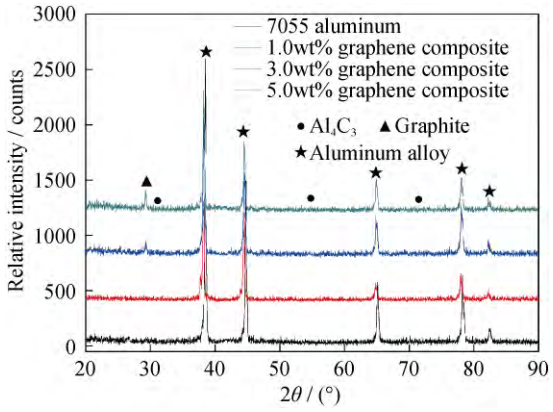


**Fig. 5. X-ray diffraction spectra of 7055 aluminum alloy and the graphene-reinforced composites.**

In this work, the sizes of metal powders and graphene plates are relatively large (micron-scale). Better dispersion of the graphene plates and further improvement of the mechanical properties can be expected if the sizes of the metal powders and graphene plates are decreased to nano-scale. In addition, the content of added graphene in this work is relatively high compared to some works [4,6]; however, the improved mechanical properties are still obtained, due to the excellent sintering and densifying abilities of SPS.

## 4. Conclusion

SPS is used to prepare graphene-reinforced 7055 aluminum alloy composites. A clean and strong interface by metallurgical bonding on an atomic scale is formed between the graphene plates and the metal matrix due to the surface cleaning and electrical activation effects of SPS, which is beneficial to improve the mechanical properties of composites. Detrimental aluminum carbide ($Al_4C_3$) is not formed during SPS processing because of the low sintering temperature and non-milling blending process. The hardness, compressive strength, and yield strength of the composites are significantly improved with 1wt% graphene addition. Further addition of graphene (3wt% and 5wt%) deteriorates the mechanical properties of the composites owing to the agglomeration of graphene plates. SPS is an excellent technique to prepare high quality graphene-reinforced metal matrix composites.

## Acknowledgements

This work was financially supported by the National Natural Science Foundation of China (No. 51271012).

## References

[1] M.A. Rafiee, J. Rafiee, Z. Wang, H.H. Song, Z.Z. Yu, and N. Koratkar, Enhanced mechanical properties of nanocomposites at low graphene content, *ACS Nano*, 3(2009), No. 12, p. 3884.

[2] Y.X. Tang, X.M. Yang, R.R. Wang, and M.X. Li, Enhancement of the mechanical properties of graphene-copper composites with graphene-nickel hybrids, *Mater. Sci. Eng. A*, 599(2014), p. 247.

[3] A.A. Balandin, S. Ghosh, W.Z. Bao, I. Calizo, D. Teweldebrhan, F. Miao, and C.N. Lau, Superior thermal conductivity of single-layer graphene, *Nano Lett.*, 8(2008), No. 3, p. 902.

[4] S.F. Bartolucci, J. Paras, M.A. Rafiee, J. Rafiee, S. Lee, D. Kapoor, and N. Koratkar, Graphene-aluminum nanocomposites, *Mater. Sci. Eng. A*, 528(2011), No. 27, p. 7933.

[5] R. Pérez-Bustamante, D. Bolaños-Morales, J. Bonilla-Martínez, I. Estrada-Guel, and R. Martínez-Sánchez, Microstructural and hardness behavior of graphene-nanoplatelets/aluminum composites synthesized by mechanical alloying, *J. Alloys Compd.*, 615(2014), Suppl 1, p. S578.

[6] J.L. Li, Y.C. Xiong, X.D. Wang, S.J. Yan, C. Yang, W.W. He, J.Z. Chen, S.Q. Wang, X.Y. Zhang, and S.L. Dai, Microstructure and tensile properties of bulk nanostructured aluminum/graphene composites prepared via cryomilling, *Mater. Sci. Eng. A*, 626(2015), p. 400.

[7] M. Rashad, F.S. Pan, A.T. Tang, M. Asif, and M. Aamir, Synergetic effect of graphene nanoplatelets (GNPs) and multi-walled carbon nanotube (MW-CNTs) on mechanical properties of pure magnesium, *J. Alloys Compd*., 603(2014), p. 111.

[8] C. Jeon, Y. Jeong, J. Seo, H.N. Tien, S. Hong, Y. Yum, S. Hur, and K. Lee, Material properties of graphene/aluminum metal matrix composites fabricated by friction stir processing, *Int. J. Precis. Eng. Manuf.*, 15(2014), No. 6, p. 1235.

[9] B. Lee, M.Y. Koo, S.H. Jin, K.T. Kim, and S.H. Hong, Simultaneous strengthening and toughening of reduced graphene oxide/alumina composites fabricated by molecular-level mixing process, *Carbon*, 78(2014), p. 212.

[10] J. Dutkiewicz, P. Ozga, W. Maziarz, J. Pstruś, B. Kania, P. Bobrowski, and J. Stolarska, Microstructure and properties of bulk copper matrix composites strengthened with various kinds of graphene nanoplatelets, *Mater. Sci. Eng. A*, 628(2015), p. 124.

[11] Y. Chang, D. Huang, C. Jia, Z. Cui, C. Wang, and D. Liang, Influence of plasma on the densification mechanism of SPS under multi-field effect, *Int. J. Miner. Metall. Mater*., 21(2014), No. 9, p. 906.

[12] J.H. Nie, C.C. Jia, N. Shi, Y.F. Zhang, Y. Li, and X. Jia, Aluminum matrix composites reinforced by molybdenum-coated carbon nanotubes, *Int. J. Miner. Metall. Mater*., 18(2011), No. 6, p. 695.

[13] M. Bastwros, G. Kim, C. Zhu, K. Zhang, S. Wang, X. Tang, and X. Wang, Effect of ball milling on graphene reinforced Al6061 composite fabricated by semi-solid sintering, *Compos. Part B*, 60(2014), p. 111.

[14] M. Fattahi, A.R. Gholami, A. Eynalvandpour, E. Ahmadi, Y. Fattahi, and S. Akhavan, Improved microstructure and mechanical properties in gas tungsten arc welded aluminum joints by using graphene nanosheets/aluminum composite filler wires, *Micron*, 64(2014), p. 20.

[15] L.Y. Chen, H. Konishi, A. Fehrenbacher, C. Ma, J.Q. Xu, H. Choi, H.F. Xu, F.E. Pfefferkorn, and X.C. Li, Novel nanoprocessing route for bulk graphene nanoplatelets reinforced metal matrix nanocomposites, *Scripta Mater.*, 67(2012), No. 1, p. 29.

[16] Y. Li, W. Liu, V. Ortalan, W.F. Li, Z. Zhang, R. Vogt, N.D. Browning, E.J. Lavernia, and J.M. Schoenung, HRTEM and EELS study of aluminum nitride in nanostructured Al 5083/$B_4C$ processed via cryomilling, *Acta Mater*., 58(2010), No. 5, p. 1732.

[17] H.G.P. Kumar and M.A. Xavior, Graphene reinforced metal matrix composite (GRMMC): a review, *Procedia Eng*., 97(2014), p. 1033.

[18] X. Jiang, M. Galano, and F. Audebert, Extrusion textures in Al, 6061 alloy and 6061/$SiC_p$ nanocomposites, *Mater. Charact*., 88(2014), p. 111.

[19] A.J. Knowles, X. Jiang, M. Galano, and F. Audebert, Microstructure and mechanical properties of 6061 Al alloy based composites with SiC nanoparticles, *J. Alloys Compd.*, 615(2014), Suppl 1, p. S401.

[20] V. Umasankar, M. Anthony Xavior, and S. Karthikeyan, Experimental evaluation of the influence of processing parameters on the mechanical properties of SiC particle reinforced AA6061 aluminium alloy matrix composite by powder processing, *J. Alloys Compd*., 582(2014), p. 380.

[21] R. Abhik, V. Umasankar, and M.A. Xavior, Evaluation of properties for Al–SiC reinforced metal matrix composite for brake pads, *Procedia Eng*., 97(2014), p. 941.

[22] P. Gao, C.C. Jia, W.B. Cao, C.C. Wang, D. Liang, and G.L. Xu, Dielectric properties of spark plasma sintered AlN/SiC composite ceramics, *Int. J. Miner. Metall. Mater*., 21(2014), No. 6, p. 589.

[23] L.H. Liu, F. Li, N. Chen, H.M. Qiu, G.H. Cao, and Y. Li, Influence of sintering temperature on the thermoelectric properties of $Ba_8Ga_{16}Si_{30}$ clathrate treated by spark plasma sintering, *Int. J. Miner. Metall. Mater*., 22(2015), No. 1, p. 78.

[24] A. Atrian, G.H. Majzoobi, M.H. Enayati, and H. Bakhtiari, Mechanical and microstructural characterization of Al7075/SiC nanocomposites fabricated by dynamic compaction, *Int. J. Miner. Metall. Mater*., 21(2014), No. 3, p. 295.

[25] N. Saheb, Spark plasma and microwave sintering of Al6061 and Al2124 alloys, *Int. J. Miner. Metall. Mater*., 20(2013), No. 2, p. 152.